IBRO Neuroscience Reports 10 (2021) 18–30

Contents lists available at ScienceDirect

IBRO Neuroscience Reports

journal homepage: www.sciencedirect.com/journal/IBRO-Neuroscience-Reports

Research Paper

Intracisternal administration of tanshinone IIA-loaded nanoparticles leads to reduced tissue injury and functional deficits in a porcine model of ischemic stroke

Elizabeth S. Waters [a,b,c,1], Erin E. Kaiser [a,b,1], Xueyuan Yang [d,1], Madison M. Fagan [a,c], Kelly M. Scheulin [a,b,c], Julie H. Jeon [e], Soo K. Shin [a,c,g], Holly A. Kinder [a,b,c], Anil Kumar [d], Simon R. Platt [a,f], Kylee J. Duberstein [a,c], Hea Jin Park [e], Jin Xie [a,d], Franklin D. West [a,b,c,g,*]

[a] Regenerative Bioscience Center, University of Georgia, Athens, GA 30602, United States
[b] Biomedical and Health Sciences Institute, University of Georgia, Athens, GA 30602, United States
[c] Department of Animal and Dairy Science, College of Agricultural and Environmental Sciences, University of Georgia, Athens, GA 30602, United States
[d] Department of Chemistry, Franklin College of Arts and Sciences, University of Georgia, Athens, GA 30602, United States
[e] Department of Foods and Nutrition, College of Family and Consumer Sciences, University of Georgia, Athens, GA 30602, United States
[f] Department of Small Animal Medicine and Surgery, College of Veterinary Medicine, University of Georgia, Athens, GA 30602, United States
[g] Interdisciplinary Toxicology Program, College of Pharmacy, University of Georgia, Athens, GA 30602, United States

ARTICLE INFO

Keywords:
Ischemic stroke
Pig stroke model
Tanshinone IIA
PLGA nanoparticle
Nanomedicine

ABSTRACT

Background: The absolute number of new stroke patients is annually increasing and there still remains only a few Food and Drug Administration (FDA) approved treatments with significant limitations available to patients. Tanshinone IIA (Tan IIA) is a promising potential therapeutic for ischemic stroke that has shown success in pre-clinical rodent studies but lead to inconsistent efficacy results in human patients. The physical properties of Tan-IIA, including short half-life and low solubility, suggests that Poly (lactic-co-glycolic acid) (PLGA) nanoparticle-assisted delivery may lead to improve bioavailability and therapeutic efficacy. The objective of this study was to develop Tan IIA-loaded nanoparticles (Tan IIA-NPs) and to evaluate their therapeutic effects on cerebral pathological changes and consequent motor function deficits in a pig ischemic stroke model.

Results: Tan IIA-NP treated neural stem cells showed a reduction in SOD activity in in vitro assays demonstrating antioxidative effects. Ischemic stroke pigs treated with Tan IIA-NPs showed reduced hemispheric swelling when compared to vehicle only treated pigs (7.85 ± 1.41 vs. 16.83 ± 0.62%), consequent midline shift (MLS) (1.72 ± 0.07 vs. 2.91 ± 0.36 mm), and ischemic lesion volumes (9.54 ± 5.06 vs. 12.01 ± 0.17 cm^3) when compared to vehicle-only treated pigs. Treatment also lead to lower reductions in diffusivity (−37.30 ± 3.67 vs. −46.33 ± 0.73%) and white matter integrity (−19.66 ± 5.58 vs. −30.11 ± 1.19%) as well as reduced hemorrhage (0.85 ± 0.15 vs 2.91 ± 0.84 cm^3) 24 h post-ischemic stroke. In addition, Tan IIA-NPs led to a reduced percentage of circulating band neutrophils at 12 (7.75 ± 1.93 vs. 14.00 ± 1.73%) and 24 (4.25 ± 0.48 vs 5.75 ± 0.85%) hours post-stroke suggesting a mitigated inflammatory response. Moreover, spatiotemporal gait deficits including

List of abbreviations: FDA, Food and Drug Administration; ICH, intracerebral hemorrhage; Tan IIA, Tanshinone IIA; PLGA, Poly (lactic-co-glycolic acid); Tan IIA-NPs, Tan IIA-loaded nanoparticles; tPA, Tissue plasminogen activator; NP, nanoparticle; ROS, reactive oxygen species; DAMPS, damaged-associated molecular patterns; TNF-α, tumor necrosis factor α; IL-6, interleukin 6; PEG–PLGA, polyethyleneglycol–polylactic-*co*-glycolic acid; BBB, blood brain barrier; CSF, cerebral spinal fluid; CNS, central nervous system; STAIR, Stroke Therapy Academic and Industry Roundtable; WM, white matter; GM, gray matter; GABA, γ-aminobutyric acid; Tan IIA-NPs, Tan IIA PLGA NPs; MLS, midline shift; PLGA-b-PEG-OH, poly (lactide-*co*-glycolide)-b-poly (ethylene glycol)-maleimide; Piog, Pioglitazone; Baic, Baicalin; Puer, Puerarin; Edar, Edaravone; Resv, Resveratrol; TEM, transmission electron microscopy; PBS, phosphate buffered saline; SOD, superoxide dismutase; IC, inhibitory concentration; UGA, University of Georgia; IM, intramuscular; TD, transdermal; MCA, middle cerebral artery; MCAO, middle cerebral artery occlusion; T2FLAIR, T2 Fluid Attenuated Inversion Recovery; T2W, T2Weighted; T2*, T2Star; DWI, Diffusion-Weighted Imaging; DTI, Diffusion Tensor Imaging; ADC, Apparent Diffusion Coefficient; FA, fractional anisotropy; ddH_2O, double-distilled water; ANOVA, analysis of variance; AU, arbitrary units; NSCs, neural stem cells; LPS, lipopolysaccharide; DLS, dynamic light scattering.

* Corresponding author at: Regenerative Bioscience Center, University of Georgia, Athens, GA 30602, United States.
E-mail address: westf@uga.edu (F.D. West).
[1] these authors contributed equally to this work.

https://doi.org/10.1016/j.ibneur.2020.11.003
Received 13 October 2020; Accepted 27 November 2020

cadence, cycle time, step time, swing percent of cycle, stride length, and changes in relative mean pressure were less severe post-stroke in Tan IIA-NP treated pigs relative to control pigs.
Conclusion: The findings of this proof of concept study strongly suggest that administration of Tan IIA-NPs in the acute phase post-stroke mitigates neural injury likely through limiting free radical formation, thus leading to less severe gait deficits in a translational pig ischemic stroke model. With stroke as one of the leading causes of functional disability in the United States, and gait deficits being a major component, these promising results suggest that acute Tan IIA-NP administration may improve functional outcomes and the quality of life of many future stroke patients.

1. Introduction

The absolute number of new stroke patients has increased to an estimated 10.3 million people a year (Benjamin et al., 2019). Unfortunately, there are few Food and Drug Administration (FDA)-approved treatments for ischemic stroke with each possessing potential risk factors. Tissue plasminogen activator (tPA), for example, has a limited administration window with potentially deadly risk factors including intracerebral hemorrhage (ICH) (Jilani and Siddiqui, 2019). The limited therapeutic time window results in relatively low administration rates (<5% patients) of tPA. There is a clear need for further investigation of novel stroke therapies and delivery approaches that lead to robust recovery. Therapeutic approaches that modulate key processes in the secondary injury cascade including inflammation and oxidative stress are promising neuroprotective options (Durukan and Tatlisumak, 2007). Tan IIA is one such neuroprotectant that acts as a free-radical scavenger and has antioxidant and anti-inflammatory effects post-stroke (Han et al., 2008; Chen et al., 2017). Tan IIA has been shown to downregulate expression of IL-1β and TNF-α and inhibit microglia activation, as well as reverse oxidative stress and apoptosis post-brain injury (Zhang et al., 2015; Chen et al., 2018; Maione et al., 2018 Huang et al., 2020). Similar to many other neuroprotective therapeutics, administration of Tan IIA has resulted in reduced lesion volumes, reduced edema, and blood brain barrier permeability. These tissue level changes resulted in decreased mortality and improved neurological function in preclinical rodent studies of neural injury (Lam et al., 2003; Tang et al., 2010; Huang et al., 2020). However, Tan IIA and many other neuroprotective therapies have demonstrated limited efficacy in human clinical trials (Sze et al., 2005; Wu et al., 2007). One potential way to improve the efficacy of Tan IIA in humans is through the use of a nanoparticle (NP) delivery system. NP drug delivery can improve drug circulation time and control release over extended periods of time while simultaneously reducing toxicity (Danhier et al., 2012). The disconnect in neuroprotectant success between preclinical rodent studies and clinical trials is likely in part due to major differences in size, cytoarchitecture, and physiology between rodent and human brains leading to dissimilar therapeutic responses (Kaur et al., 2013; Cai and Wang, 2016). These inherent anatomical differences have led to a demand from the stroke therapeutic community for the development and testing of novel treatments in more representative translational animal models, such as the pig, that more closely resemble human brain anatomy and physiology (Stroke Therapy Academic Industry, 1999; Baker et al., 2017).

Following the primary ischemic insult, a secondary injury cascade is initiated with the release of the excitatory neurotransmitter, glutamate, from dying neurons causing excitotoxicity, peri-infarct depolarizations, production of reactive oxygen species (ROS), and inflammation (Endres et al., 2009; Bernstock et al., 2017). Generated ROS leads to the damage of DNA, RNA, and critical cellular machinery leading to cell death. The increase in ROS, the release of damaged-associated molecular patterns (DAMPS), and hypoxia triggers an immune response including an increase in neutrophils and the production of inflammatory cytokines such as tumor necrosis factor α (TNF-α) and interleukin 6 (IL-6) (Rothwell and Hopkins, 1995; Dirnagl et al., 1999). The secondary injury cascade leads to rapid and substantial brain damage. Therefore, inhibiting ROS production and inflammation may be a promising therapeutic target.

Tan IIA has been shown to have antioxidant and anti-inflammatory effects in rodent and human stroke studies (Tang et al., 2014). Rodent studies showed Tan IIA was effective in reducing brain edema and infarct volume in response to ischemic injury (Lam et al., 2003; Tang et al., 2010, 2014). Reduced brain edema and lesioning correlated with rodent improvements in overall neurological function post-stroke including limb mobility, ambulation, righting reflexes, and reduced circling behavior (Lam et al., 2003). Clinical trials testing Tan IIA in its purified or crude form (dried *Salvia miltiorhiza* root) has led to mixed efficacy results with studies showing significant to no improvements in clinical outcomes (e.g. cerebral blood flow, neurological symptoms, and muscle strength) of ischemic stroke patients (Zhou et al., 2005; Wu et al., 2007). Conflicting results between rodent and human outcomes suggest Tan IIA may be a potentially effective treatment, yet further optimization is needed to achieve improved consistency in post-stroke outcomes.

In its purified form, Tan IIA has a short circulation half-life and poor solubility, which limits systemic drug concentrations and consequent pharmacological responses (Chen et al., 2007; Savjani et al., 2012). Furthermore, the hydrophobic properties of Tan IIA reduces permeability and bioavailability, thus requiring higher administration doses (Savjani et al., 2012). Polylactic-*co*-glycolic acid (PLGA) NPs are an FDA-approved copolymer made of lactic acid and glycolic acid. PLGA or the PEGylated derivative, polyethyleneglycol–polylactic-*co*-glycolic acid (PEG–PLGA), can encapsulate large amounts of hydrophobic molecules, like Tan IIA, and release them at a controlled rate (Locatelli and Comes Franchini, 2012). A sustained drug release improves drug bioavailability and reduces the frequency of drug administration. The controlled release, low toxicity, high biodegradability, low immunogenicity, and significant clinical experience makes PLGA a favorable nanoplatform for drug delivery (Govender et al., 1999). Extensive preclinical and clinical studies confirm PLGA NPs are a safe and efficient delivery system (Danhier et al., 2012; Locatelli and Comes Franchini, 2012). A PLGA NP delivery system could significantly improve the bioavailability, solubility, and pharmacological efficacy of Tan IIA in ischemic stroke patients. NP treatments are commonly delivered intravenously (IV), however this limits the therapeutic effects of NP delivered drugs for ischemic stroke as NPs cannot freely transverse the blood brain barrier (BBB). Intracisternal delivery of NPs may overcome this challenge as NPs do not need to cross the BBB due to direct administration into the cerebral spinal fluid (CSF) of the central nervous system (CNS). Additionally, intracisternal NP treatments are not diluted in the circulatory system, removed by filtering organs such as the liver, thus lower NP concentrations are required, and the potential of off target effects in other organ systems is reduced.

The Stroke Therapy Academic and Industry Roundtable (STAIR) recommended preclinical testing of potential therapeutics in gyrencephalic species to increase the possibility of translating therapies to the clinic (Stroke Therapy Academic Industry, 1999). The use of large animal models is an important step in the translational framework as most therapies that have reached and failed in clinical trials have been successfully tested in rodent models, indicating a need for a more predictive model. The pig has anatomical and physiological similarities to humans making it a robust model for studying novel therapeutics for ischemic stroke (Lind et al., 2007). While rodent brains are lissencephalic and composed of <12% white matter (WM), both human and pig

brains are gyrencephalic and composed of >60% WM (Nakamura et al., 2009). These differences have proven critically important in ischemic stroke pathology as WM and gray matter (GM) exhibit differing sensitivities to hypoxia, with WM more consistently injured in most stroke cases (McKay et al., 2007; Baltan et al., 2008). The pathology of GM is believed to differ from WM in terms of lymphocyte infiltration, macrophage activity, and BBB alterations in response to injury (Mallucci et al., 2015). WM also has a greater dependence on Na^+ and Ca^{2+} exchange, γ-aminobutyric acid (GABA), and adenosine with an autoprotective feed-back loop (Fern et al., 1994). These anatomical similarities support that stroke pathophysiology in the pig model is likely more representative of the human condition and therefore more predictive of human outcomes compared to traditional rodent models.

In this proof of concept study, Tan IIA PLGA NPs (Tan IIA-NPs) were characterized and demonstrated antioxidative and anti-inflammatory capabilities in vitro. Acute testing of Tan IIA-NPs in a pig model of ischemic stroke showed Tan IIA-NPs have a neuroprotective effect leading to reduced cerebral swelling, lesion volume, and improved WM integrity. These tissue level improvements corresponded with improved motor function suggesting Tan IIA-NPs may be an effective treatment for ischemic stroke.

2. Materials and methods

The overarching aim of this study was to characterize and evaluate Tan IIA-NPs and their efficacy as a potential acute stroke therapy in a clinically relevant pig model of ischemic stroke. Tan IIA-NPs were synthesized and characterized. Ischemic stroke was induced, and Tan IIA-NPs were delivered intracisternally as single dose 1 h post-stroke induction. MRI was performed 24 h post-stroke. Venous blood was collected pre-stroke, 4, 12, and 24 h post-stroke. Gait analysis was performed pre and 48 h post-stroke. Only two animals were included in each treatment group for a total of 4 animals for in vivo studies, therefore statistical analysis was limited to in vitro studies.

2.1. Synthesis of PLGA-b-PEG-OH

PLGA acid (PLGA-COOH;1.0 g, 0.170 mmol, Mn = 7000; Lactel), polyethylene glycol (HO-PEG-OH;2.29 g, 0.684 mmol, Mn = 2000; Sigma Aldrich), and deoxyadenosine monophosphate (dMAP; 0.023 g, 0.187 mmol; Alfa Aesar) were dissolved in 30 mL of anhydrous dichloromethane (CH_2Cl_2; Sigma Aldrich). Next, a 10 mL CH_2Cl_2 solution of dicyclohexylmethanediimine (DCC; 0.141 g or 0.684 mmol; Sigma Aldrich) was added dropwise to the reaction mixture at 0 °C with magnetic stirring. The mixture was warmed up to room temperature and stirred overnight. Insoluble dicyclohexylurea ($C_{13}H_{24}N_2O$) was filtered out. The raw product was precipitated out by adding 50 mL of 50:50 diethyl ether ($(C_2H_5)_2O$; Sigma Aldrich) and methanol (CH_3OH; Sigma Aldrich) to the mixture. The mixture was centrifuged for 15 min at 4 °C. The purification step was repeated 4–5 times, followed by ^1H NMR analysis that was performed on a Varian Mercury Plus 400 system.

2.2. NP synthesis

PLGA NPs were synthesized through a nanoprecipitation method. Briefly, poly (lactide-*co*-glycolide)-b-poly (ethylene glycol)-maleimide (PLGA-b-PEG-OH) was first dissolved in dimethylformamide (DMF) at a concentration of 50 mg/mL. 100 μL of the polymer solution was mixed with drug-to-be-loaded (150 μL, 0.15 mg; Tan IIA, TCI America; Piog, Sigma Aldrich; Baic, Sigma Aldrich; Puer, Sigma Aldrich; Edar, Sigma Aldrich; Resv, Sigma Aldrich) for 30% feeding and diluted with DMF (Fisher Scientific) to a final polymer concentration of 5 mg/mL. The mixture was added dropwise to sterile nanopure water with constant stirring, and the resulting solution was agitated in a fume hood for 2 h. Drug loaded NPs were collected on an amicon ultracentrifugation unit (100 kDa cut-off) and were washed 3–4 times with water. Finally, the NPs were resuspended in sterilized nanopure water.

2.3. NP characterizations

A drop of diluted NP solution was deposited onto a transmission electron microscopy (TEM) grid, followed by staining with 2% uranyl acetate. TEM images were taken on a FEI Tecnai 20 transmission electron microscope operating at an accelerating voltage of 200 kV. Hydrodynamic size and surface charge of NPs were analyzed on a Malvern Zetasizer Nano ZS system.

2.4. Drug loading and release

For drug loading analysis, a 50 μL aqueous solution of NPs was diluted to 900 μL and 100 μL 0.1 mM sodium hydroxide (NaOH; Sigma Adrich) was added to the solution. The mixture was incubated at room temperature overnight. Next, the solution was sonicated for 30 min and centrifugated at 5000 rpm for 10 min. 100 μL supernatant was transferred into a 96-well UV transparent plate and its absorbance at the relevant wavelength was measured (Tan IIA: 258 nm; Baic: 320 nm; Piog: 270 nm). To test drug release, 100 μL NP solution was loaded onto a dialysis unit and allowed to float on a 1.1 mL PBS solution (pH: 5.5, 6.5, or 7.4; Gibco). The system was put on an Eppendorf shaker set at 37 °C. At each time point (0.5, 1, 2, 4, 8, 12, 24, 36, and 48 h), 100 μL PBS solution was transferred to a 96-well UV transparent plate. The drug content was assessed by measuring the relevant absorbance (Tan IIA: 258 nm; Baic: 320 nm; Piog: 270 nm) and compared to a standard curve. 100 μL of fresh PBS solution was added back to the dialysis system.

2.5. Cell culture

Neural stem cells (NSCs; HIP™ hNSC BC1, GlobalStem) were maintained on Matrigel-coated (Corning) tissue culture treated plates in NSC media composed of Neurobasal medium (Gibco), 2% B-27 Supplement (Gibco), 1% non-essential amino acids (Gibco) 2 mM L-glutamine (Gibco), 1% penicillin/streptomycin (Gibco), 20 ng/mL basic fibroblast growth factor (bFGF; R&D Systems). NSCs were incubated at 37 °C with 5% CO_2 and a complete media change was performed every other day. When NSCs reached confluence, cells were enzymatically passaged using Accutase (Gibco).

Microglia cells (ATCC) were maintained on tissue culture treated plates in microglia media composed of Eagle's Minimum Essential Medium (ATCC), 11% fetal bovine serum (ATCC) 1% penicillin/streptomycin (Gibco). Microglia were incubated at 37 °C with 5% CO_2 and a complete media change was performed every other day. When microglia reached confluence, cells were enzymatically passaged using 0.05% trypsin (Gibco).

2.6. MTT assay

The MTT assay was performed according to the manufacturer's protocol (Sigma Aldrich). Briefly, 8×10^3 NSCs were seeded into each well of a 96 well plate. After 8 h of incubation at 37 °C in a humidified atmosphere with 5% CO_2, a gradient of the tested drugs or NPs were added into the wells. After 24 h of incubation, the medium was removed, and cells were washed. 10 μL MTT solution (10 mg/mL) was added into each well and incubated with cells for 4 h. The absorbance at 570 nm was measured on a plate reader. Viability was calculated by computing relative absorbance with regard to PBS treated cells.

2.7. SOD activity assay

The SOD activity assay was performed according to the manufacturer's protocol (Cayman). Briefly, 1×10^6 NSCs were seeded into each well of a 6-well plate. After 24 h, the cells were incubated with 250 μM hydrogen peroxide (H_2O_2) to induce oxidative stress. After 30 min, the

cells were washed with PBS and then incubated with drugs or drug-containing NPs at different concentrations for 24 h. The cells were then detached from plate using a cell scraper, collected by centrifugation, and washed 3 times with PBS. The resultant cells were homogenized by sonication and then centrifuged at 3600 rpm at 4 °C for 10 min. The supernatant was immediately collected and diluted with assay buffers by 4 times the supernatant amount. The diluted solutions were transferred into a 96-well plate at a volume of 200 μL per well. 20 μL of diluted xanthine oxidase was added into the solution and the plate was covered with foil and shaken at room temperature for 30 min. The absorbance at 450 nm was then read on a plate reader. The SOD activity was calculated as μ/mL of protein by comparing to SOD standards.

2.8. ELISA assays

Anti-inflammatory efficacy was tested by TNF-α and IFN-γ enzyme-linked immunosorbent assay (ELISA) assays according to the manufacturer's protocol (Invitrogen). Briefly, 2×10^4 microglia cells in microglia media were seeded in 12 well plates overnight. To induce an inflammatory response in microglia cells, 150 ng/mL LPS was added in each well and incubated at 37 °C with 5% CO_2. After 24 h, cells were washed with PBS 2 times and then incubated with either drugs or at each respective drugs IC 20, IC 6.7, IC 2.2, IC 0.74, IC 0.25 or 0 based on the previously performed MTT assay and 150 ng/mL LPS. Negative control samples were not treated with LPS or drug. After 24 h, supernatant was collected from each well, processed and absorbance was read at 450 nm. Cytokine values were calculated as pg/mL.

2.9. Animals and housing

All work performed in this study was approved by the University of Georgia (UGA) Institutional Animal Care and Use Committee (IACUC; Protocol Number: 2017–07–019Y1A0) and in accordance with the National Institutes of Health Guide for the Care and Use of Laboratory Animals guidelines to ensure appropriate and humane use of animals. Sexually mature, castrated male Landrace pigs, 5–6 months old and 48–56 kg were enrolled in this study. Male pigs were used in accordance with the STAIR guidelines that suggests initial therapeutic evaluations should be performed with young, healthy male animals (Lapchak et al., 2013). Pigs were individually housed at a room temperature approximately 27 ºC with a 12-hour light/dark cycle. All pigs were fed standard grower diets.

2.10. MCAO and NP delivery

One day prior to surgery, antibiotics and pain medication were administered (exceed; 5 mg/kg intramuscular (IM) and fentanyl patch; 100 mg/kg/hr transdermal (TD)). Pre-induction analgesia and sedation were achieved using xylazine (2 mg/kg IM) and midazolam (0.2 mg/kg IM). Anesthesia was induced with IV propofol to effect and prophylactic lidocaine (1.0 mL 2% lidocaine) topically to the laryngeal folds to facilitate intubation. Anesthesia was maintained with isoflurane (Abbott Laboratories) in oxygen.

As previously described, a curvilinear skin incision extended from the right orbit to an area rostral to the auricle (Platt et al., 2014). A segment of the zygomatic arch was resected while the temporal fascia and muscle were elevated and a craniectomy was performed exposing the local dura mater. Following a local durectomy, the distal middle cerebral artery (MCA) and associated branches were permanently occluded using bipolar cautery forceps resulting in ischemic infarction. The temporalis muscle and epidermis were routinely re-apposed.

At 1 h post-stroke, PBS (n = 2) or Tan IIA-NPs (n = 2) (total animals = 4) were intracisternally delivered via a 20 gauge, 3.5 or 6" spinal needle inserted through the skin on the midline of the dorsal neck, at an anatomical intersection of a vertical line created by the rostral aspect of the wings of the first vertebral body and a horizontal line connecting the dorsal arch of C2 with the occipital protuberance. Once the needle was through the cutaneous tissues, the stylet was removed and advanced until CSF appeared in the needle hub confirming entry into the cistern. A small volume (3–5 mLs) of CSF was removed while the spinal needle was in place and the volume removed was replaced with PBS or Tan IIA-NPs. The volume of NPs delivered was determined by the NP encapsulation efficiency and each animal received a dose of 133 μg/kg Tan IIA.

Anesthesia was discontinued, pigs were returned to their pens upon extubation, and monitored every 15 min until vitals including temperature, heart rate, and respiratory rate returned to normal. Monitoring was reduced to every 4 h for 24 h, and then twice a day thereafter until post-transplantation sutures were removed. Banamine (2.2 mg/kg IM) was administered for post-operative pain and fever management every 12 h for the first 24 h post-stroke and then every 24 h for 3 d.

2.11. MRI acquisition and analysis

MRI was performed 24 h post-stroke on a General Electric 3.0 Tesla MRI system. Pigs were sedated and maintained under anesthesia as previously described for MCA occlusion surgery. MRI of the cranium was performed using an 8-channel torso coil with pigs positioned in supine recumbency. Multiplanar MRI sequences were acquired including T2 Fluid Attenuated Inversion Recovery (T2FLAIR), T2W, T2*, Diffusion Weighted Imaging (DWI), and Diffusion Tensor Imaging (DTI). Sequences were analyzed using Osirix software (Version 5.6). Cytotoxic edema consistent with ischemic stroke was confirmed 24 h post-stroke by comparing hyperintense regions in T2FLAIR and DWI sequences to corresponding hypointense regions in DWI generated ADC maps.

Hemisphere volume was calculated using T2W sequences for each axial slice by manually outlining the ipsilateral and contralateral hemispheres, while excluding the ventricles. The hemisphere areas were multiplied by the T2W slice thickness (3 mm) to obtain total hemisphere volumes. Lesion volume was calculated using DWI sequences for each axial slice by manually outlining hyperintense regions of interest (ROI). The area of each ROI was multiplied by the DWI slice thickness (2 mm) to obtain the total lesion volume. ADC values were calculated for each axial slice based on hypointense ROI and directly compared to identical ROI in the contralateral hemisphere. DTI was utilized to generate FA maps. FA values of the internal capsules were manually calculated on the slice where the internal capsules and the splenium of the corpus callosum were visualized. FA values were expressed as a percent change in the ipsilateral hemisphere relative to the contralateral hemisphere. ICH volume was calculated based on hypointense ROIs in T2* sequences and multiplied by the slice thickness (2 mm).

2.12. Blood collection and analysis

Venous blood samples were collected pre-stroke, 4 h, 12 h, and 24 h post-stroke into K2EDTA spray coated tubes (Patterson Veterinary). Samples were stored at room temperature for 30 min. 4 μL of blood was then pipetted onto a ColorFrost microscope slide (ThermoScientific) approximately 1 cm from the bottom. A spreader slide was placed in front of the blood at a 45° angle and retracted while maintaining even pressure until the blood sample spread evenly along the width of the slide. Care was taken to ensure each blood smear covered approximately two-thirds of the slide and exhibited an oval feathered end. Each slide was air-dried for 10 min and fixed with methanol for 2 min. Once dry, the slide was stained with Rowmanosky stain for 5 min. The stained slide was then submerged in double-distilled water (ddH_2O) for 10 min. Finally, the slide was rinsed and allowed to air dry prior to applying a cover slip. Trained, blinded personnel completed manual cell counts of lymphocytes and band neutrophils at the monolayer, beginning approximately 1 mm away from the body of the smear. The first 100 cells visualized were identified and cell counts were expressed as a percentage.

2.13. Gait analysis

Pre- and post-stroke, all pigs underwent gait analysis to measure differences in spatiotemporal and relative pressure gait parameters between treatment groups. 2 weeks prior to stroke induction, all pigs were trained to travel across a gait mat at a consistent, two-beat pace. Pigs received food rewards at each end of the mat for each successful run in which the pig was not distracted and moved at a consistent pace. For each pig, pre-stroke data was collected on 3 separate days. At each time point, pigs moved across the mat until 5 consistent repetitions were achieved, with no more than 15 total repetitions collected.

All data was automatically captured using a GAITFour® electronic, pressure-sensitive mat (CIR Systems Inc., Franklin, NJ) that is 7.01 m in length and 0.85 m in width with an active area that is 6.10 m in length and 0.61 m in width. In this arrangement, the active area is a grid, 48 sensors wide by 480 sensors long, totaling 23,040 sensors. Gait data was then semi-automatically analyzed using the GAITFour® Software. All resulting data was analyzed for cadence (steps/min). Further measurements were quantified for the left forelimb, contralateral to the stroke lesion. These measurements included stride length (distance between successive ground contact of the left forelimb), swing percent of cycle (percent of a full gait cycle in which the left forelimb is not in contact with the ground), cycle time (amount of time for a full stride cycle), and mean pressure (amount of pressure exerted by the left forelimb).

2.14. Statistical analysis

All quantitative data was analyzed with SAS (Version 9.3; Cary, NC) and statistical significances between groups were determined by one-way analysis of variance (ANOVA) and post-hoc Tukey-Kramer Pair-Wise comparisons. Treatments where p-values ≤ 0.05 were considered significantly different. Only two animals were included in each treatment group for a total of 4 animals for in vivo studies, therefore statistical analysis was limited to in vitro studies.

3. Results

3.1. Tan IIA and Baicalin drug characteristics enable NP drug delivery

Six neuroprotective drugs with antioxidative and/or anti-inflammatory properties were identified, Baicalin (Baic), Pioglitazone (Piog), Tan IIA, Puerarin (Puer), Edaravone (Edar), and Resveratrol (Resv), and were selected for testing as a NP based ischemic stroke therapy. These drugs were selected based on preclinical success in treating ischemic stroke, with some advancing and proving unsuccessful in human clinical trials, while also having biological characteristics that could benefit from the use of a NP delivery system such as a short half-life (Lam et al., 2003; Wu et al., 2007; Chang et al., 2009; Tu et al., 2009, Tang et al., 2010; Blankenship et al., 2011; Tu et al., 2011; Koronowski et al., 2017, Zheng al., 2017, Lee and Xiang, 2018; Yaghi et al. 2018; Kobayashi et al. 2019). Puer, Edar, and Resv showed very low NP encapsulation efficiency (0.00%, 0.125%, and 0.132%, respectively), due to their relatively high hydrophilicity, and therefore these drugs were eliminated from the study. Baic, Piog, and Tan IIA showed higher encapsulation efficiencies of 17.01%, 4.90%, and 15.90%, respectively. Baic, Piog, and Tan IIA loaded NPs (henceforth referred to as Baic-NPs, Piog-NPs, and Tan IIA-NPs) were imaged using TEM and had an average size of 60.80, 74.20, and 52.20 nm, respectively (Fig. 1A). Baic-NPs, Piog-NPs, and Tan IIA-NPs size was also assessed by dynamic light scattering (DLS), which found the hydrodynamic sizes to be 89.28 ± 1.8, 122.40 ± 2.3, and 91.34 ± 1.3 nm, respectively (Fig. 1B). The relative increase of hydrodynamic sizes is attributed to surface PEGylation and hydration. Assessment of zeta potential showed that all three NPs have a negatively charged surface, 31.91, −27.39, −28.98 mV, respectively, which is due to the hydroxyl termini of the PEG chains (Fig. 1C). For all three formulations, the drug molecules were slowly released from NPs at acidic and more neutral pH levels (pH 5.5, 6.5, and 7.4; Fig. 1D), which is beneficial from a sustained delivery perspective. However, while Tan IIA-NPs and Baic-NPs afford good colloidal stability, Piog-NPs showed a relatively high degree of aggregation after dispersing in phosphate buffered saline (PBS) for 2–3 h. Hence, subsequent cellular tests focused on Baic-NPs and Tan IIA-NPs.

3.2. Tan IIA-NPs and Baic-NPs suppress oxidative stress in NSCs and inflammation in microglia

Tan IIA and Baic have been previously shown to be effective in ischemic stroke animal models at a dose range of 15 mg/kg and 90 mg/kg, respectively (Shang et al., 2013; Liang et al., 2017). Therefore, Tan IIA-NPs, Baic-NPs and corresponding free drugs were tested for cytotoxicity and efficacy in a comparable dose range. MTT assays were performed to determine the relative cytotoxicity of Tan IIA-NPs, Baic-NPs and corresponding free drugs on neural stem cells (NSCs). MTT assays at 24 h showed reduced viability of the cells at 33 μM of Tan IIA-NPs and 672 μM of Baic-NPs (Fig. 2A−B). Notably, while Baic-NPs showed very similar profiles to the Baic free molecules, Tan IIA-NPs showed significantly ($p < 0.05$) less toxicity compared to free Tan IIA 6.6 μM. This may be attributed to NP-mediated, slow release of Tan IIA at early timepoints.

To study the antioxidative efficacy of Tan IIA-NPs and Baic-NPs, NSCs were treated with H_2O_2 (250 μM) and incubated with drug-loaded NPs and corresponding free drugs. A series of dilutions (determined from respective inhibitory concentration $(IC)_{20}$ doses) were tested. Oxidative stress was tested by measuring superoxide dismutase (SOD) activity at 24 h (Fig. 2). Both Tan IIA-NPs and Baic-NPs showed a concentration-dependent reduction of SOD activity, indicating an anti-oxidative effect (Fig. 2C−D). Tan IIA-NPs resulted in a greater reduction in SOD levels than Baic-NPs at their respective IC_{20} (2 vs. 672 μM, respectively) and $IC_{2.5}$ (0.25 vs. 84 μM, respectively) doses.

To assess the potential anti-inflammatory effect of Tan IIA-NPs and Baic-NPs, microglia cells were treated with lipopolysaccharide (LPS) and then incubated with drug-loaded NPs and free drugs. The inflammatory response was assessed by measuring TNF-α and IFN-γ. Positive controls treated with LPS showed a significant ($p < 0.05$) increase in TNF- α and IFN-γ levels (128.03 ± 26.21 and 45.92 ± 1.02 pg/mL, respectively). Treatment of microglia with Tan IIA-NPs and Baic-NPs at IC_{20} and $IC_{2.5}$ doses resulted in undetectable levels of TNF-α and IFN-γ. The absence of TNF-α and IFN-γ after treatment with Tan IIA-NPs and Baic-NPs demonstrates these NPs have an anti-inflammatory response in vitro (data not shown). Based on these combined cytotoxicity, oxidative stress, and inflammatory test results, Tan IIA-NPs were selected for further testing in an ischemic stroke pig model.

3.3. Tan IIA-NPs reduce hemispheric swelling, consequent MLS, and ischemic lesion volumes post-ischemic stroke

T2Weighted (T2W) sequences collected 24 h post-stroke revealed Tan IIA-NP treated pigs (Fig. 3B) exhibited a reduced percent change in ipsilateral hemispheric swelling when compared to PBS controls (Fig. 3A) (7.85 ± 1.41 vs. 16.83 ± 0.62%, respectively; Fig. 3C). This mitigation of hemispheric swelling resulted in a decreased MLS (1.72 ± 0.07 vs. 2.91 ± 0.36 mm; red lines; Fig. 3D). Acute ischemic lesion volumes were also reduced in Tan IIA-NP treated pigs 24 h post-stroke (9.54 ± 5.06 vs. 12.01 ± 0.17 cm^3; Fig. 3E), which suggests a reduction in acute tissue injury.

3.4. Tan IIA-NP treatment leads to reduced cytotoxic edema, WM damage, and ICH post-ischemic stroke

Hypointense lesioned areas were observed on Apparent Diffusion Coefficient (ADC) maps, which are indicative of restricted diffusion and cytotoxic edema (Fig. 4A−B, white arrows). Tan IIA-NP treated pigs

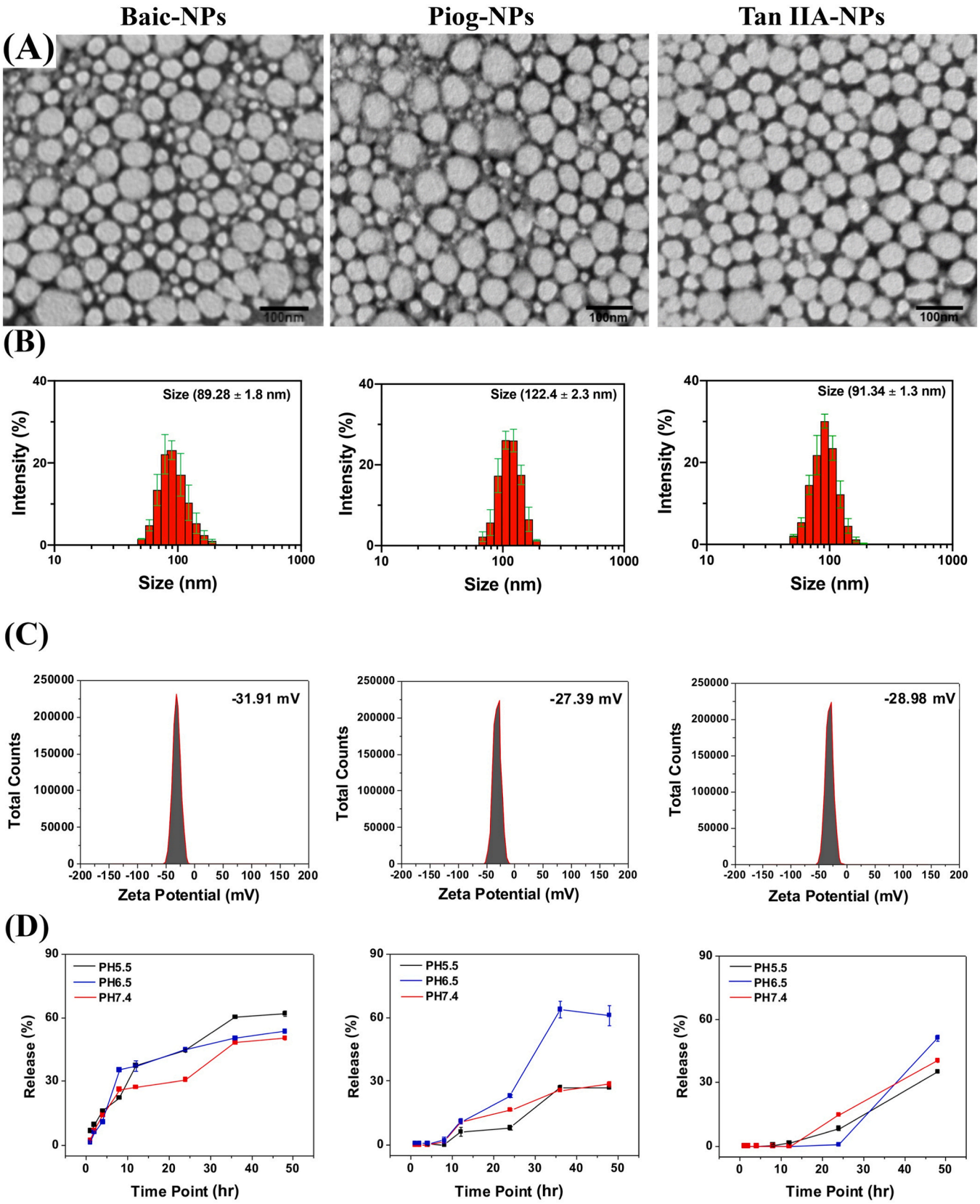

Fig. 1. Baic, Piog, and Tan IIA are capable of undergoing NP packaging. TEM images of drug loaded PLGA NPs (A). The average NP sizes were 60.8, 74.2, and 52.2 nm for Baic-NPs, Piog-NPs, and Tan IIA-NPs, respectively. Hydrodynamic sizes of NPs were 89.28 ± 1.8, 122.4 ± 2.3, and 91.34 ± 1.3 nm for Baic-NPs, Piog-NPs, and Tan IIA-NPs, respectively (B). NPs zeta potentials were −31.91, −27.39, and −28.98 mV for Baic-NPs, Piog-NPs, and Tan IIA-NPs, respectively (C). Drug release profiles for Baic-NPs, Piog-NPs, and Tan IIA-NPs (**D**).

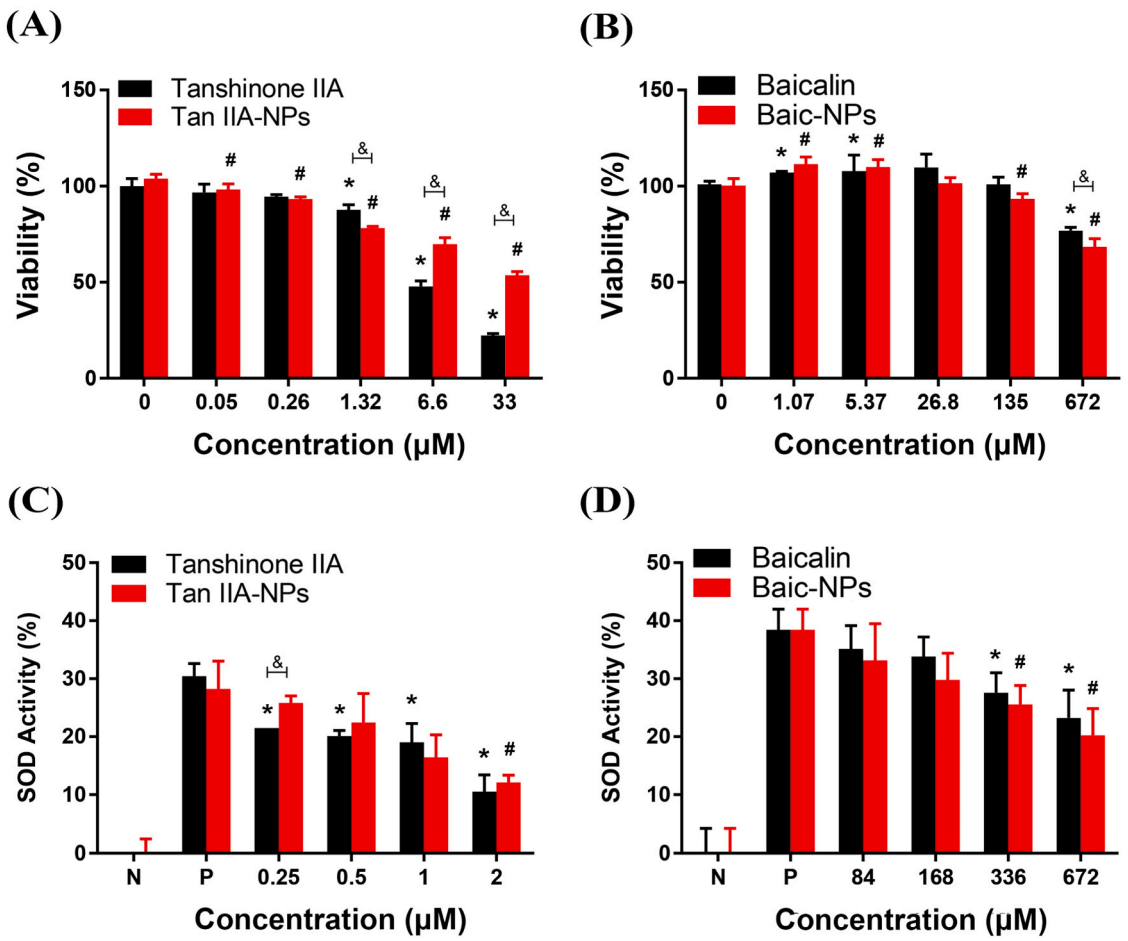

Fig. 2. Tan IIA-NPs show significantly reduced toxicity in NSCs than freeform drug and Tan IIA-NPs and Baic-NPs reduce oxidative stress in NSCs. MTT assays at 24 h showed reduced viability of the cells at 33 μM of Tan IIA-NPs and 672 μM of Baic-NPs (Fig. 2A–B). * or # indicates a significant difference between vehicle only control and treatment. & indicates a significant difference between drug only and drug loaded NP. SOD assay results showed a significant reduction in SOD at 2 μM and 336 μM for Tan IIA-NPs (C) and Baic-NPs (D), respectively. * or # indicates a significant difference between positive control and treatment. & indicates a significant difference between drug only and drug loaded NP. (N = negative control, P = positive control).

(Fig. 4B) had a reduced percent change in mean ADC values when compared PBS control pigs (Fig. 4A) (−37.30 ± 3.67 vs. −46.33 ± 0.73%; Fig. 4C). To determine the neuroprotective effect of Tan IIA-NPs on cerebral WM, internal capsule fractional anisotropy (FA) values were evaluated in Tan IIA-NP and PBS treated animals at 24 h post-stroke. Tan IIA-NP treated animals showed a decreased reduction in FA value relative to PBS treated animals (−19.66 ± 5.58 vs. −30.11 ± 1.19%; Fig. 4D). T2Star (T2*) sequences showed hypointense acute ICH in PBS and Tan IIA-NP treated pigs 24 h post-stroke (Fig. 5A–B, respectively). However, Tan IIA-NP treated pigs had smaller hemorrhage volumes compared to PBS treated pigs (0.85 ± 0.15 vs 2.91 ± 0.84 cm^3; Fig. 5C). This data supports that Tan IIA-NPs lead to a reduction in restricted diffusion, cytotoxic edema, WM damage, and ICH in ischemic stroke animals.

3.5. *Tan IIA-NPs reduce circulating band neutrophils in post-stroke pigs*

To assess changes in the stroke immune response, band neutrophil and lymphocyte populations were measured in blood samples collected pre-stroke, 4, 12, and 24 h post-stroke. At 12 h post-stroke, the percentage of circulating band neutrophils was lower in Tan IIA-NP treated animals than in the PBS control animals at 12 (7.75 ± 1.93 vs. 14.00 ± 1.73%) and 24 (4.25 ± 0.48 vs 5.75 ± 0.85%) post-stroke (Fig. S1B). Conversely, the percentage of circulating lymphocytes was similar in both treatment groups at all assessed time points (Fig. S1C–D).

3.6. *Spatiotemporal and kinetic gait deficits are less severe post-stroke in Tan IIA-NP treated pigs*

Changes in key spatiotemporal and kinetic gait parameters were measured to detect differences in functional outcomes post-Tan IIA-NP treatment. A decrease was noted for both treatment groups in the average cadence of the pigs from pre-stroke to post-stroke indicating a decrease in speed. However, the decrease in cadence was more severe for the PBS treated pigs compared to Tan IIA-NP treated pigs (133.9 ± 2.71–64.8 ± 5.86steps/min vs. 135.7 ± 7.08–109.98 ± 0.00steps/min, respectively, Fig. 6A). The limb contralateral to the stroke lesion is often more affected as compared to the ipsilateral limb, which in this study are the limbs of the left side. In addition, pigs typically carry more weight on the forehand, typically making deficits more severe in the left forelimb. Deficits were noted for the left forelimb in both treatment groups for multiple gait parameters. The cycle time of the left front limb increased post-stroke for both treatment groups, with a more drastic increase in cycle time noted for the PBS treatment group as compared to the Tan IIA-NP treated pigs (0.46 ± 0.02–0.94 ± 0.08 vs. 0.44 ± 0.02–0.55 ± 0.00 s, respectively, Fig. 6B). Similarly, the left front step time increased post-stroke in both groups, with a greater increased step time in PBS pigs compared to Tan IIA-NP pigs (0.24 ± 0.01–0.49 ± 0.07 vs. 0.22 ± 0.01–0.27 ± 0.00 s,

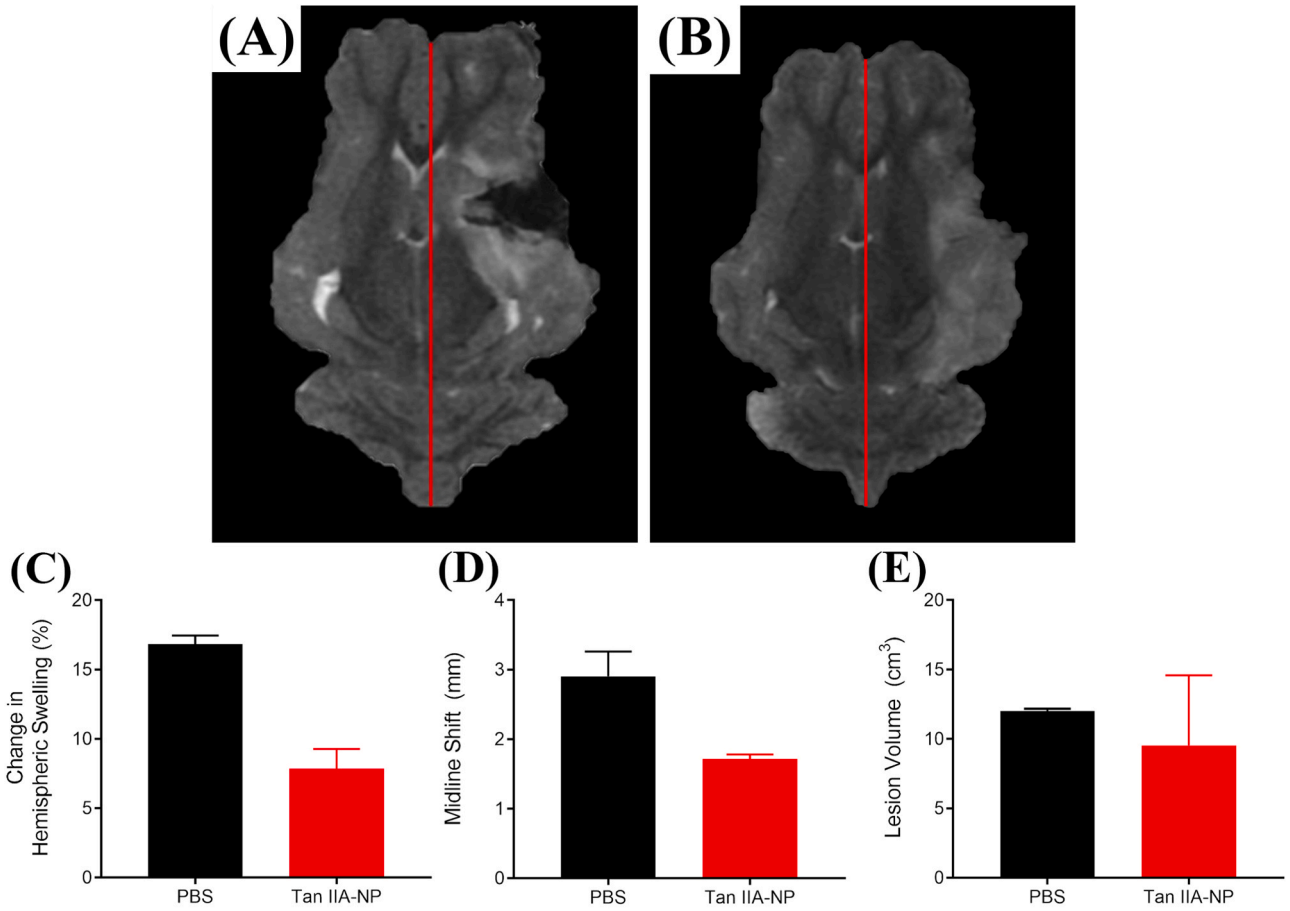

Fig. 3. Tan IIA-NPs reduce hemispheric swelling, MLS, and ischemic lesion volumes. Compared to PBS pigs (n = 2) (A), Tan IIA-NP treated pigs (n = 2) (B) exhibited a reduction in ipsilateral hemispheric swelling (7.85 ± 1.41 vs. 16.83 ± 0.62%, respectively; C), MLS (1.72 ± 0.07 vs. 2.91 ± 0.36 mm mm, respectively, red lines; D), and lesion volumes (9.54 ± 5.06 vs. 12.01 ± 0.17 cm^3, respectively; E) at 24 h post-stroke.

respectively, Fig. 6C). Decreases in cycle time and step time indicated an overall slower gait post-stroke, opposed to pre-stroke performance. The swing percent of cycle decreased for the left front limb of all pigs, with PBS pigs decreasing further than Tan IIA-NP pigs (49.4 ± 0.26–33.3 ± 1.77 vs. 49.1 ± 1.90–43.2 ± 0.00%, respectively, Fig. 6D). A reduction was noted in the left front stride length of all animals, with PBS pigs displaying a greater reduction in stride length relative to Tan IIA-NP pigs (78.38 ± 2.37–63.19 ± 3.94 vs. 84.87 ± 1.78–77.44 ± 0.00 cm, respectively, Fig. 6E). Finally, the mean pressure of the left front limb decreased in both treatment groups with a larger decrease in pressure noted for the PBS pigs opposed to the Tan IIA-NP pigs (2.93 ± 0.03–2.67 ± 0.03 vs. 2.87 ± 0.03–2.88 ± 0.00 arbitrary units (AU), respectively, Fig. 6F). Post-stroke deficits were noted for all parameters in both treatment groups, however more pronounced deficits were seen in the gait of PBS pigs, thus indicating administration of Tan IIA-NP in the acute phase post-stroke leads to less severe gait deficits.

4. Discussion

In this study, we demonstrate for the first time Tan IIA-NP treatment leads to improvements in clinically relevant MRI-based stroke tissue injury parameters and functional deficits in a translational ischemic stroke pig model. Tan IIA-NP therapy was selected from a number of drug candidates based on in vitro assessment of biochemical properties that augment NP delivery of a drug and efficacy in antioxidative and anti-inflammatory studies. Tan IIA-NP therapy resulted in considerable reductions in MLS, lesion volumes, WM damage, and ICH in the pig stroke model; parameters that closely correlate with functional deficits and mortality in human patients (Hacke et al., 1996; Berrouschot et al., 1998; Falcao et al., 2004). Tan IIA-NP treatment and associated reduction in overall brain injury corresponded with less severe spatiotemporal and relative pressure gait deficits including parameters that are often affected in human patients including stride length and cadence (Hsu et al., 2003; Balaban and Tok, 2014). These promising preclinical results in the pig model suggest that Tan IIA-NP therapy is ready for the next step in the STAIR criteria for translating pre-clinical studies into human clinical trials including expanded studies with additional animals of both genders and therapeutic window and dose finding studies.

To improve drug bioavailability, Tan IIA was encapsulated into PLGA-PEG NPs. The nanoplatform allows for controlled release of Tan IIA, potentially leading to prolonged ant-inflammatory and oxidative effects. In addition, Tan IIA-NPs were injected intracisternal into the subarachnoid space rather than IV. This injection route bypasses the BBB that would otherwise prevent the delivery of therapeutics to the ischemic areas. Combining NP delivery and intracisternal administration represents a novel approach in drug delivery. A recent study performed in mice also observed efficient distribution and good tolerance of NPs after intracisternal injection (Householder et al., 2019). Because the entire CNS can be accessed through the CSF, this approach may be extended for the treatment of other CNS diseases.

Infarct volume, cerebral swelling, and consequent MLS have been shown to play a key role in the development of neurological deficits and high patient mortality rates (Hacke et al., 1996; Berrouschot et al., 1998; Thrift et al., 2000; Tang et al., 2010). In the present study, the acute treatment window of Tan IIA-NPs demonstrated potential in mitigating

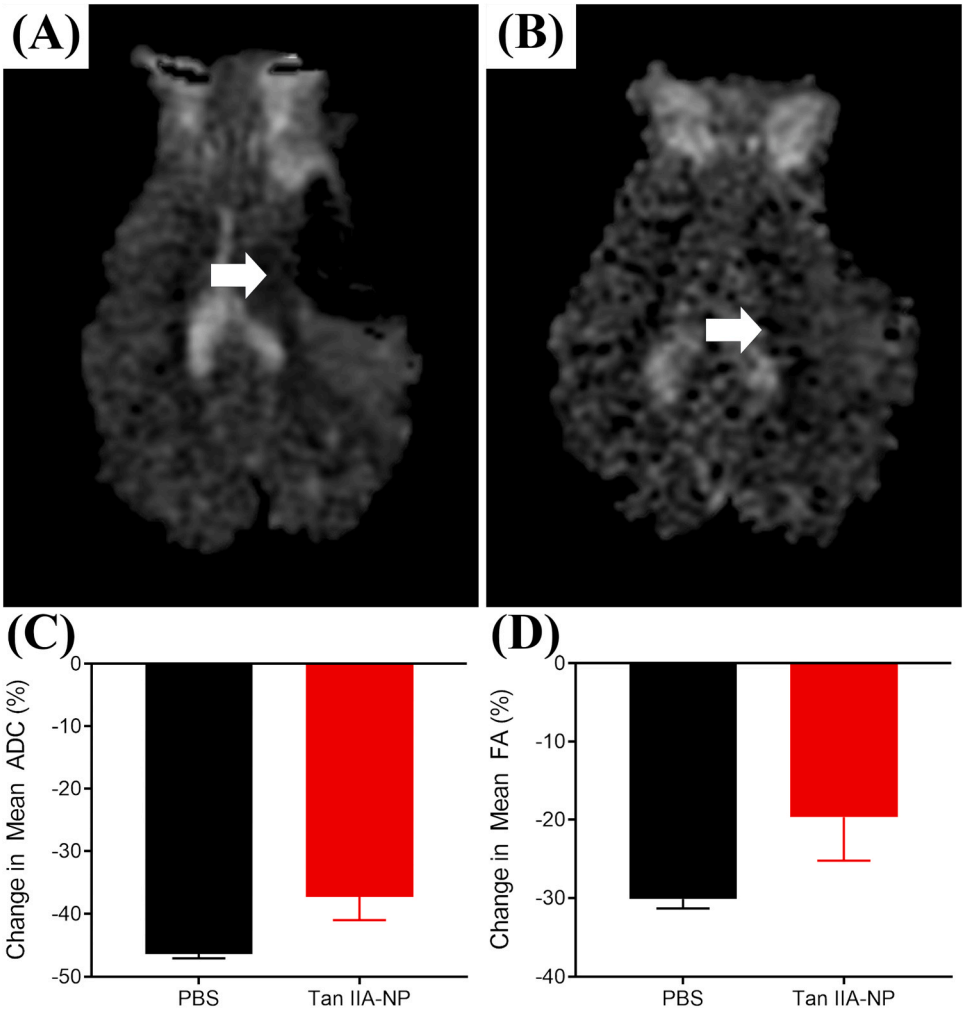

Fig. 4. Tan IIA-NPs lead to reduced cytotoxic edema and WM damage post-ischemic stroke. Hypointense lesioned areas were observed on ADC maps in PBS (n = 2) (A) and Tan IIA-NP (n = 2) (B) treated pigs. Tan IIA-NP treated pigs had a smaller percent change in mean ADC relative to PBS treated pigs (−37.30 ± 3.67 vs. −46.33 ± 0.73%, respectively; C). Treated pigs showed a decreased reduction in FA values relative to PBS treated pigs (−19.66 ± 5.58 vs. −30.11 ± 1.19%, respectively; D).

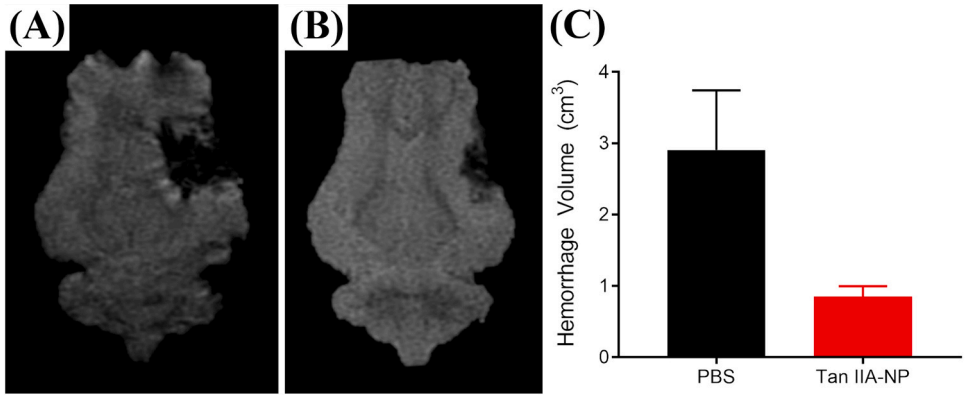

Fig. 5. Tan IIA-NPs lead to reduced hemorrhage post-ischemic stroke. T2* sequences showed acute ICH in PBS (n = 2) (A) and Tan IIA-NP (n = 2) (B) treated pigs 24 h post-stroke. Tan IIA-NP treated pigs had smaller hemorrhage volumes compared to PBS treated pigs (0.85 ± 0.15 vs 2.91 ± 0.84 cm^3, respectively; C).

these clinical presentations by decreasing hemisphere and lesion volumes. In a study of free form Tan IIA, Tang et al. provided evidence that lesion volumes were significantly reduced in 1 and 4 h post-stroke Tan IIA treatment groups versus 6 and 12 h Tan IIA treatment groups in their rat study of ischemic stroke (Tang et al., 2014). Additional studies have indicated Tan IIA possesses a neuroprotective effect in cerebral ischemia-reperfusion rodent models, whereby encephaledema and hemispheric swelling were relieved, infarction volumes decreased, and neurobehavior scores were significantly improved (Liu et al., 2010; Wang et al., 2010).

Measures of ICH and ADC and are also strong predictors of clinical outcomes with increased hemorrhage and decreased ADC values being closely associated with poor clinical outcomes and higher mortality rates (Terruso et al., 2009; Beslow et al., 2011). In the current study, Tan IIA-NP treated animals showed a decreased hemorrhage volume and a decreased percent change in ADC values relative to PBS treated animals.

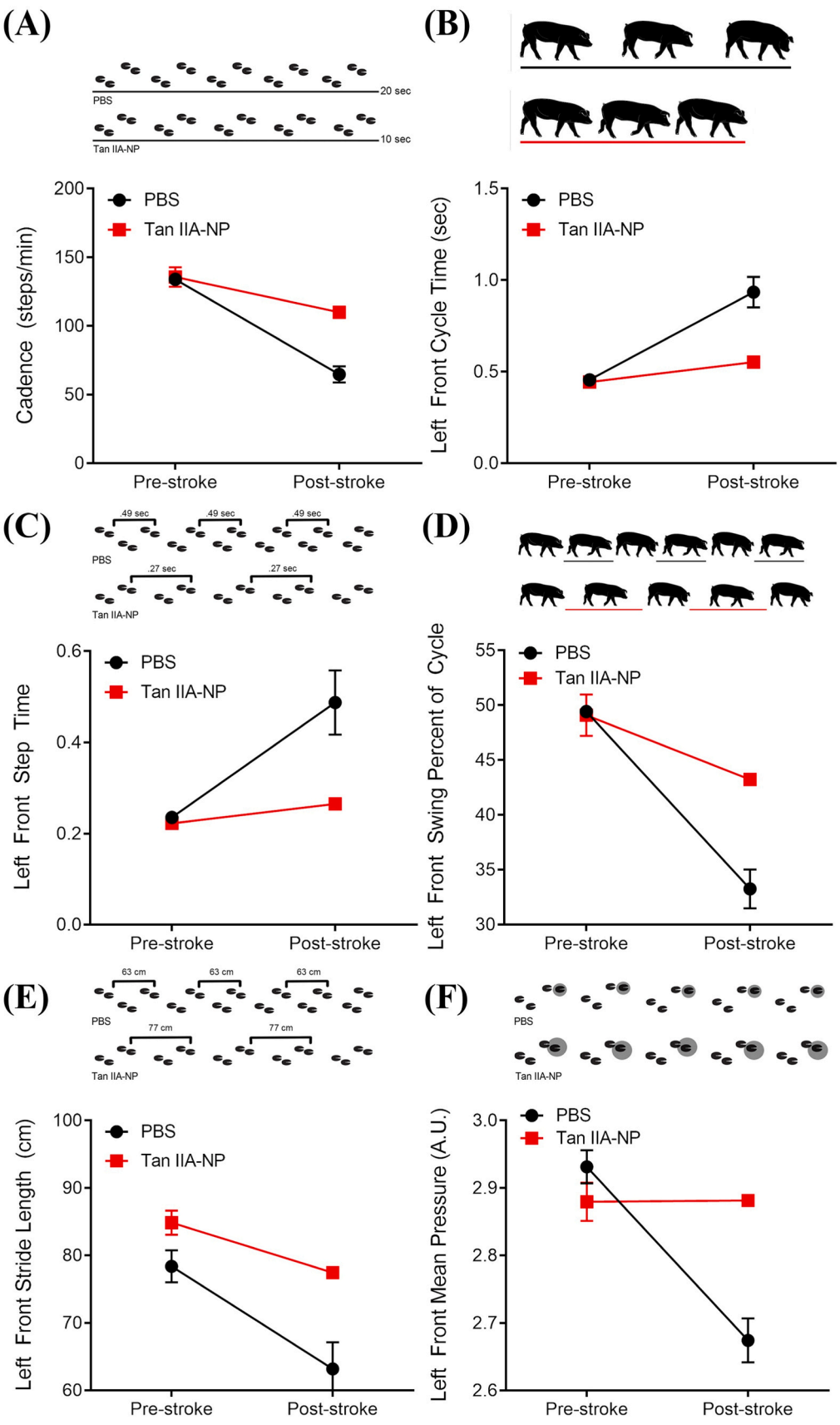

Fig. 6. Spatiotemporal and kinetic gait deficits are less severe post-stroke in Tan IIA-NP treated pigs. A decrease in the average cadence of the pigs from pre-stroke to post-stroke was more severe in PBS control pigs opposed to Tan IIA-NP treated pigs (133.9 ± 2.71–64.8 ± 5.86steps/min vs. 135.7 ± 7.08–109.98 ± 0.00steps/min, respectively; A). The cycle time of the left front limb increased more drastically in PBS control pigs as compared to Tan IIA-NP treated pigs (0.46 ± 0.02–0.94 ± 0.08 vs. 0.44 ± 0.02–0.55 ± 0.00 s, respectively; B). The left front step time increased post-stroke in PBS pigs more so than Tan IIA-NP pigs (0.24 ± 0.01–0.49 ± 0.07 vs. 0.22 ± 0.01–0.27 ± 0.00 s, respectively; C). The swing percent of cycle decreased more for the left front limb of PBS control pigs than Tan IIA-NP pigs (49.4 ± 0.26–33.3 ± 1.77 vs. 49.1 ± 1.90–43.2 ± 0.00%, respectively; D). The left front stride length of pigs treated with PBS displaying a greater reduction in stride length relative to Tan IIA-NP pigs (78.38 ± 2.37–63.19 ± 3.94 vs. 84.87 ± 1.78–77.44 ± 0.00 cm, respectively; E). A larger decrease in mean pressure of the left front limb was noted for PBS control pigs but not Tan IIA-NP treated pigs (2.93 ± 0.03–2.67 ± 0.03 vs. 2.87 ± 0.03–2.88 ± 0.00 AU, respectively; F).

A recent study in a middle cerebral artery occlusion (MCAO) ischemic stroke mouse model showed that free form Tan IIA has a protective effect on the BBB, which would result in reduced hemorrhage (Wang et al., 2010). This study demonstrated increased presence of the tight junction protein claudin-5 and reduced BBB leakage in Tan IIA treated animals. In a study assessing the ability of Tan IIA to maintain vascular integrity in a rat aneurysm model, researchers demonstrated Tan IIA reduced aneurysm size and increased vascular wall thickness improving vascular integrity relative to control animals (Ma et al., 2019). Zhou et al. showed in an ICH zebrafish model, Tan IIA reduced ICH area and incidence (Zhou et al., 2018). In a follow-up in vitro study with human umbilical vein endothelial cells, they demonstrated that Tan IIA inhibits actin depolymerization near cell borders and cell contraction, which would result in destabilization of cell-cell adheren junctions critical to maintaining the BBB. These results in multiple unique disease models across three different species demonstrates Tan IIA leads to increased stability in intracerebral vasculature that would result in reduced ICH as observed in this study. Preservation of diffusivity observed in this study is likely a direct result of decreased injury due to acute Tan IIA-NP treatment. This corresponds with previous Tan IIA studies in rodent models showing improved cerebral blood flow, reduced free radical formation, inflammation, and a decrease in infarcted brain tissue (Lam et al. 2003; Tang et al. 2014).

Gait deficits constitute a significant portion of disabilities related to stroke. Unsurprisingly, many patients report improvement in mobility as a main goal for post-stroke recovery, making this an important benchmark for stroke therapeutic treatment potential (Cress and Fleming, 1966). Human stroke patients are often left with hemiparesis resulting in gait deficits including decreased cadence and stride length with associated increased swing percent of cycle and cycle time (Balaban and Tok, 2014). Similarly, pigs in the current study exhibited a post-stroke decrease in stride length and cadence with an associated increase in cycle time and step time in the left forelimb. These alterations in gait patterns mirror what is seen in humans and are likely reflective of the decreased velocity that typically accompanies postural instability following stroke. Further, pigs in the current study showed decreased swing percent of cycle of the affected contralateral forelimb post-stroke. While this is opposite of what is often seen in human stroke patients, a decrease in relative swing and increase in relative stance has been reported as a hallmark gait change in pig models for both stroke and traumatic brain injury and is likely due to an increased need for ground contact to stabilize the gait along with decreased propulsion (Duberstein et al., 2014; Baker et al., 2019; Kinder et al., 2019). In the present study, changes in spatiotemporal gait properties were noted in all pigs in the acute time frame following stroke, however a more pronounced deficit was noted in the gait of PBS pigs as compared to Tan IIA-NP pigs post-stroke. Additionally, PBS pigs in this study also showed a reduction in mean hoof pressure of the contralateral forelimb, indicating compensatory balance mechanisms to distribute weight away from the affected contralateral side, while Tan IIA-NP pigs showed no kinetic changes. Several studies have demonstrated Tan IIA administration in rodent stroke models led to a reduction in severity of functional neurologic deficits (determined by factors such as failure to extend the forepaw of the contralateral limb, circling, lack of balance, or inability to walk) as compared to control animals (Lam et al., 2003; Chen et al., 2012). The results of the present study are in agreement with these rodent models and suggest the administration of Tan IIA-NPs in the acute phase post-stroke mitigates cerebral injury and thereby results in less severe functional deficits.

5. Conclusion

This proof of concept study demonstrated Tan IIA-NPs have notable potential to be a novel treatment for ischemic stroke. Utilizing a highly translatable pig model of ischemic stroke, Tan IIA-NP treatment leads to reduced hemispheric swelling, MLS, lesion volumes, cytotoxic edema, WM damage, and ICH 24 h post-stroke. These manifested improvements in acute ischemic stroke pathophysiology led to marked improvements in a number of spatiotemporal and kinetic gait parameters. These promising results support the idea Tan IIA-NPs are ready for further preclinical studies assessing safety and efficacy in a larger cohort of animals in both sexes in order to evaluate dosing and administration windows in accordance with the STAIR criteria for therapeutic translation to clinical trials.

Ethics approval and consent to participate

All work performed in this study was approved by the UGA Institutional Animal Care and Use Committee (IACUC; Protocol Number: 2017–07–019Y1A0) and in accordance with the National Institutes of Health Guide for the Care and Use of Laboratory Animals guidelines to ensure appropriate and humane use of animals.

Consent for publication

Not applicable.

Availability of data and materials

The datasets used and/or analyzed during the current study are available from the corresponding author on reasonable request.

Funding

This work was supported by the National Institutes of Health, National Institute of Neurological Disorders and Stroke, USA grant R01NS093314.

CRediT authorship contributions statement

Elizabeth S. Waters and Erin E. Kaiser assisted in experimental design, performed animal experiments, analyzed and interpreted data, and were major contributors in manuscript writing. Xueyuan Yang and Anil Kumar performed nanoparticle experiments, analyzed and interpreted data, and were contributors in manuscript writing. Madison M. Fagan performed gait and behavior testing, data analysis and interpretation and was a major contributor in manuscript writing. Holly A. Kinder, Kelly M. Scheulin, Soo K. Shin, and Julie H. Jeon assisted in planning, animal care, and data collection. Simon R. Platt performed animal surgeries. Kylee J. Duberstein, Hea Jin Park, Jin Xie, and Franklin D. West led experimental design, analyzed and interpreted data, and were major contributors in manuscript writing. All authors read and approved the final manuscript.

Acknowledgments

The authors would like to thank Brandy Winkler and our team of undergraduate researchers who were involved in various aspects of surgeries, post-operative care, pig gait/behavioral testing, and data analysis. We would also like to thank the UGA Animal Resources team for veterinary care and guidance as well as Rick Utley and Kelly Parham for their pig expertise and management skills. We would like to thank Samantha Spellicy for her assistance with midline shift and blood analysis.

Competing interests

The authors declare that they have no competing interests.

Appendix A. Supporting information

Supplementary data associated with this article can be found in the

online version at doi:10.1016/j.ibneur.2020.11.003.

References

Baker, E.W., Kinder, H.A., Hutcheson, J.M., Duberstein, K.J.J., Platt, S.R., Howerth, E.W., West, F.D., 2019. Controlled cortical impact severity results in graded cellular, tissue, and functional responses in a piglet traumatic brain injury model. J Neurotrauma 36 (1), 61–73.

Baker, E.W., Platt, S.R., Lau, V.W., Grace, H.E., Holmes, S.P., Wang, L., Duberstein, K.J., Howerth, E.W., Kinder, H.A., Stice, S.L., Hess, D.C., Mao, H., West, F.D., 2017. Induced pluripotent stem cell-derived neural stem cell therapy enhances recovery in an ischemic stroke pig model. Sci. Rep. 7 (1), 10075.

Balaban, B., Tok, F., 2014. Gait disturbances in patients with stroke. PM R 6 (7), 635–642.

Baltan, S., Besancon, E.F., Mbow, B., Ye, Z., Hamner, M.A., Ransom, B.R., 2008. White matter vulnerability to ischemic injury increases with age because of enhanced excitotoxicity. J. Neurosci. 28 (6), 1479–1489.

Benjamin, E.J., Muntner, P., Alonso, A., Bittencourt, M.S., Callaway, C.W., Carson, A.P., Chamberlain, A.M., Chang, A.R., Cheng, S., Das, S.R., Delling, F.N., Djousse, L., Elkind, M.S.V., Ferguson, J.F., Fornage, M., Jordan, L.C., Khan, S.S., Kissela, B.M., Knutson, K.L., Kwan, T.W., Lackland, D.T., Lewis, T.T., Lichtman, J.H., Longenecker, C.T., Loop, M.S., Lutsey, P.L., Martin, S.S., Matsushita, K., Moran, A.E., Mussolino, M.E., O'Flaherty, M., Pandey, A., Perak, A.M., Rosamond, W.D., Roth, G. A., Sampson, U.K.A., Satou, G.M., Schroeder, E.B., Shah, S.H., Spartano, N.L., Stokes, A., Tirschwell, D.L., Tsao, C.W., Turakhia, M.P., VanWagner, L.B., Wilkins, J. T., Wong, S.S., Virani, S.S., American Heart Association Council on, E., Prevention Statistics, C., Stroke Statistics, S., 2019. Heart disease and stroke statistics-2019 update: a report from the American Heart Association. Circulation 139 (10), e56–e528.

Bernstock, J.D., Peruzzotti-Jametti, L., Ye, D., Gessler, F.A., Maric, D., Vicario, N., Lee, Y. J., Pluchino, S., Hallenbeck, J.M., 2017. Neural stem cell transplantation in ischemic stroke: a role for preconditioning and cellular engineering. J. Cereb. Blood Flow Metab. 37 (7), 2314–2319.

Berrouschot, J., Sterker, M., Bettin, S., Koster, J., Schneider, D., 1998. Mortality of space-occupying ('malignant') middle cerebral artery infarction under conservative intensive care. Intensive Care Med. 24 (6), 620–623.

Beslow, L.A., Smith, S.E., Vossough, A., Licht, D.J., Kasner, S.E., Favilla, C.G., Halperin, A.R., Gordon, D.M., Jones, C.I., Cucchiara, A.J., Ichord, R.N., 2011. Hemorrhagic transformation of childhood arterial ischemic stroke. Stroke 42 (4), 941–946.

Blankenship, D., Niemi, J., Hilow, E., Karl, M., Sundararajan, S., 2011. Oral pioglitazone reduces infarction volume and improves neurologic function following MCAO in rats. Adv. Exp. Med. Biol. 701, 157–162.

Cai, B., Wang, N., 2016. Large animal stroke models vs. rodent stroke models, pros and cons, and combination? Acta Neurochir. Suppl. 121, 77–81.

Chang, Y., Hsieh, C.Y., Peng, Z.A., Yen, T.L., Hsiao, G., Chou, D.S., Chen, C.M., Sheu, J. R., 2009. Neuroprotective mechanisms of puerarin in middle cerebral artery occlusion-induced brain infarction in rats. J. Biomed. Sci. 16, 9.

Chen, J., Bi, Y., Chen, L., Zhang, Q., Xu, L., 2018. Tanshinone IIA exerts neuroprotective effects on hippocampus-dependent cognitive impairments in diabetic rats by attenuating ER stress-induced apoptosis. Biomed. Pharmacother. 104, 530–536.

Chen, H.S., Qi, S.H., Shen, J.G., 2017. One-compound-multi-target: combination prospect of natural compounds with thrombolytic therapy in acute ischemic stroke. Curr. Neuropharmacol. 15 (1), 134–156.

Chen, Y., Wu, X., Yu, S., Fauzee, N.J., Wu, J., Li, L., Zhao, J., Zhao, Y., 2012. Neuroprotective capabilities of Tanshinone IIA against cerebral ischemia/reperfusion injury via anti-apoptotic pathway in rats. Biol. Pharm. Bull. 35 (2), 164–170.

Chen, X., Zhou, Z.W., Xue, C.C., Li, X.X., Zhou, S.F., 2007. Role of P-glycoprotein in restricting the brain penetration of tanshinone IIA, a major active constituent from the root of Salvia miltiorrhiza Bunge, across the blood-brain barrier. Xenobiotica 37 (6), 635–678.

Cress, R.H., Fleming, W.C., 1966. Treatment goals and selection of patients for rehabilitation with hemiplegia. Ala J. Med. Sci. 3 (3), 307–311.

Danhier, F., Ansorena, E., Silva, J.M., Coco, R., Le Breton, A., Preat, V., 2012. PLGA-based nanoparticles: an overview of biomedical applications. J. Control Release 161 (2), 505–522.

Dirnagl, U., Iadecola, C., Moskowitz, M.A., 1999. Pathobiology of ischaemic stroke: an integrated view. Trends Neurosci. 22 (9), 391–397.

Duberstein, K.J., Platt, S.R., Holmes, S.P., Dove, C.R., Howerth, E.W., Kent, M., Stice, S. L., Hill, W.D., Hess, D.C., West, F.D., 2014. Gait analysis in a pre- and post-ischemic stroke biomedical pig model. Physiol. Behav. 125, 8–16.

Durukan, A., Tatlisumak, T., 2007. Acute ischemic stroke: overview of major experimental rodent models, pathophysiology, and therapy of focal cerebral ischemia. Pharmacol. Biochem. Behav. 87 (1), 179–197.

Endres, M., Dirnagl, U., Moskowitz, M.A., 2009. The ischemic cascade and mediators of ischemic injury. Handb. Clin. Neurol. 92, 31–41.

Falcao, A.L., Reutens, D.C., Markus, R., Koga, M., Read, S.J., Tochon-Danguy, H., Sachinidis, J., Howells, D.W., Donnan, G.A., 2004. The resistance to ischemia of white and gray matter after stroke. Ann. Neurol. 56 (5), 695–701.

Fern, R., Waxman, S.G., Ransom, B.R., 1994. Modulation of anoxic injury in CNS white matter by adenosine and interaction between adenosine and GABA. J. Neurophysiol. 72 (6), 2609–2616.

Govender, T., Stolnik, S., Garnett, M.C., Illum, L., Davis, S.S., 1999. PLGA nanoparticles prepared by nanoprecipitation: drug loading and release studies of a water soluble drug. J. Controll. Release 57 (2), 171–185.

Hacke, W., Schwab, S., Horn, M., Spranger, M., De Georgia, M., von Kummer, R., 1996. "Malignant' middle cerebral artery territory infarction: clinical course and prognostic signs. Arch. Neurol. 53 (4), 309–315.

Han, J.Y., Fan, J.Y., Horie, Y., Miura, S., Cui, D.H., Ishii, H., Hibi, T., Tsuneki, H., Kimura, I., 2008. Ameliorating effects of compounds derived from Salvia miltiorrhiza root extract on microcirculatory disturbance and target organ injury by ischemia and reperfusion. Pharmacol. Ther. 117 (2), 280–295.

Householder, K.T., Dharmaraj, S., Sandberg, D.I., Wechsler-Reya, R.J., Sirianni, R.W., 2019. Fate of nanoparticles in the central nervous system after intrathecal injection in healthy mice. Sci. Rep. 9 (1), 12587.

Hsu, A.L., Tang, P.F., Jan, M.H., 2003. Analysis of impairments influencing gait velocity and asymmetry of hemiplegic patients after mild to moderate stroke. Arch. Phys. Med. Rehabil. 84 (8), 1185–1193.

Huang, Y., Long, X., Tang, J., Li, X., Zhang, X., Luo, C., Zhou, Y., Zhang, P., 2020. The attenuation of traumatic brain injury via inhibition of oxidative stress and apoptosis by Tanshinone IIA. Oxid. Med. Cell Longev. 2020, 4170156.

Jilani, T.N. and A.H. Siddiqui, 2019. Tissue plasminogen activator. StatPearls. Treasure Island (FL).

Kaur, H., Prakash, A., Medhi, B., 2013. Drug therapy in stroke: from preclinical to clinical studies. Pharmacology 92 (5–6), 324–334.

Kinder, H.A., Baker, E.W., Wang, S., Fleischer, C.C., Howerth, E.W., Duberstein, K.J., Mao, H., Platt, S.R., West, F.D., 2019. Traumatic brain injury results in dynamic brain structure changes leading to acute and chronic motor function deficits in a pediatric piglet model. J. Neurotrauma.

Kobayashi, S., Fukuma, S., Ikenoue, T., Fukuhara, S., Kobayashi, S., 2019. Effect of edaravone on neurological symptoms in real-world patients with acute ischemic stroke. Stroke 50 (7), 1805–1811.

Koronowski, K.B., Khoury, N., Saul, I., Loris, Z.B., Cohan, C.H., Stradecki-Cohan, H.M., Dave, K.R., Young, J.I., Perez-Pinzon, M.A., 2017. Neuronal SIRT1 (Silent Information Regulator 2 Homologue 1) regulates glycolysis and mediates resveratrol-induced ischemic tolerance. Stroke 48 (11), 3117–3125.

Lam, B.Y., Lo, A.C., Sun, X., Luo, H.W., Chung, S.K., Sucher, N.J., 2003. Neuroprotective effects of tanshinones in transient focal cerebral ischemia in mice. Phytomedicine 10 (4), 286–291.

Lapchak, P.A., Zhang, J.H., Noble-Haeusslein, L.J., 2013. RIGOR guidelines: escalating STAIR and STEPS for effective translational research. Transl. Stroke Res. 4 (3), 279–285.

Lee, X.R., Xiang, G.L., 2018. Effects of edaravone, the free radical scavenger, on outcomes in acute cerebral infarction patients treated with ultra-early thrombolysis of recombinant tissue plasminogen activator. Clin. Neurol. Neurosurg. 167, 157–161.

Liang, W., Huang, X.B., Chen, W.Q., 2017. The effects of Baicalin and Baicalein on cerebral ischemia: a review. Aging Dis. 8 (6), 850–867.

Lind, N.M., Moustgaard, A., Jelsing, J., Vajta, G., Cumming, P., Hansen, A.K., 2007. The use of pigs in neuroscience: modeling brain disorders. Neurosci. Biobehav. Rev. 31 (5), 728–751.

Liu, L., Zhang, X., Wang, L., Yang, R., Cui, L., Li, M., Du, W., Wang, S., 2010. The neuroprotective effects of Tanshinone IIA are associated with induced nuclear translocation of TORC1 and upregulated expression of TORC1, pCREB and BDNF in the acute stage of ischemic stroke. Brain Res. Bull. 82 (3–4), 228–233.

Locatelli, E., Comes Franchini, M., 2012. Biodegradable PLGA-b-PEG polymeric nanoparticles: synthesis, properties, and nanomedical applications as drug delivery system. J. Nanopart. Res. 14 (12).

Maione, F., Piccolo, M., De Vita, S., Chini, M.G., Cristiano, C., De Caro, C., Lippiello, P., Miniaci, M.C., Santamaria, R., Irace, C., De Feo, V., Calignano, A., Mascolo, N., Bifulco, G., 2018. Down regulation of pro-inflammatory pathways by tanshinone IIA and cryptotanshinone in a non-genetic mouse model of Alzheimer's disease. Pharmacol. Res. 129, 482–490.

Mallucci, G., Peruzzotti-Jametti, L., Bernstock, J.D., Pluchino, S., 2015. The role of immune cells, glia and neurons in white and gray matter pathology in multiple sclerosis. Prog. Neurobiol. 127–128, 1–22.

Ma, J., Hou, D., Wei, Z., Zhu, J., Lu, H., Li, Z., Wang, X., Li, Y., Qiao, G., Liu, N., 2019. Tanshinone IIA attenuates cerebral aneurysm formation by inhibiting the NFkappaBmediated inflammatory response. Mol. Med. Rep. 20 (2), 1621–1628.

McKay, S.M., Brooks, D.J., Hu, P., McLachlan, E.M., 2007. Distinct types of microglial activation in white and grey matter of rat lumbosacral cord after mid-thoracic spinal transection. J. Neuropathol. Exp. Neurol. 66 (8), 698–710.

Nakamura, M., Imai, H., Konno, K., Kubota, C., Seki, K., Puentes, S., Faried, A., Yokoo, H., Hata, H., Yoshimoto, Y., Saito, N., 2009. Experimental investigation of encephalomyosynangiosis using gyrencephalic brain of the miniature pig: histopathological evaluation of dynamic reconstruction of vessels for functional anastomosis. Laboratory investigation. J. Neurosurg. Pediatr. 3 (6), 488–495.

Platt, S.R., Holmes, S.P., Howerth, E.W., Duberstein, K.J.J., Dove, C.R., Kinder, H.A., Wyatt, E.L., Linville, A.V., Lau, V.W., Stice, S.L., Hill, W.D., Hess, D.C., West, F.D., 2014. Development and characterization of a Yucatan miniature biomedical pig permanent middle cerebral artery occlusion stroke model. Exp. Transl. Stroke Med. 6 (1), 5.

Rothwell, N.J., Hopkins, S.J., 1995. Cytokines and the nervous system II: actions and mechanisms of action. Trends Neurosci. 18 (3), 130–136.

Savjani, K.T., Gajjar, A.K., Savjani, J.K., 2012. Drug solubility: importance and enhancement techniques. ISRN Pharm. 2012, 195727.

Shang, Y.H., Tian, J.F., Hou, M., Xu, X.Y., 2013. Progress on the protective effect of compounds from natural medicines on cerebral ischemia. Chin. J. Nat. Med. 11 (6), 588–595.
Stroke Therapy Academic Industry, R., 1999. Recommendations for standards regarding preclinical neuroprotective and restorative drug development. Stroke 30 (12), 2752–2758.
Sze, F.K., Yeung, F.F., Wong, E., Lau, J., 2005. Does Danshen improve disability after acute ischaemic stroke? Acta Neurol. Scand. 111 (2), 118–125.
Tang, Q., Han, R., Xiao, H., Li, J., Shen, J., Luo, Q., 2014. Protective effect of tanshinone IIA on the brain and its therapeutic time window in rat models of cerebral ischemia-reperfusion. Exp. Ther. Med. 8 (5), 1616–1622.
Tang, C., Xue, H., Bai, C., Fu, R., Wu, A., 2010. The effects of Tanshinone IIA on blood-brain barrier and brain edema after transient middle cerebral artery occlusion in rats. Phytomedicine 17 (14), 1145–1149.
Terruso, V., D'Amelio, M., Di Benedetto, N., Lupo, I., Saia, V., Famoso, G., Mazzola, M.A., Aridon, P., Sarno, C., Ragonese, P., Savettieri, G., 2009. Frequency and determinants for hemorrhagic transformation of cerebral infarction. Neuroepidemiology 33 (3), 261–265.
Thrift, A.G., Dewey, H.M., Macdonell, R.A., McNeil, J.J., Donnan, G.A., 2000. Stroke incidence on the east coast of Australia: the North East Melbourne Stroke Incidence Study (NEMESIS). Stroke 31 (9), 2087–2092.
Tu, X.K., Yang, W.Z., Liang, R.S., Shi, S.S., Chen, J.P., Chen, C.M., Wang, C.H., Xie, H.S., Chen, Y., Ouyang, L.Q., 2011. Effect of baicalin on matrix metalloproteinase-9 expression and blood-brain barrier permeability following focal cerebral ischemia in rats. Neurochem. Res. 36 (11), 2022–2028.
Tu, X.K., Yang, W.Z., Shi, S.S., Wang, C.H., Chen, C.M., 2009. Neuroprotective effect of baicalin in a rat model of permanent focal cerebral ischemia. Neurochem. Res. 34 (9), 1626–1634.
Wang, L., Zhang, X., Liu, L., Cui, L., Yang, R., Li, M., Du, W., 2010. Tanshinone II A down-regulates HMGB1, RAGE, TLR4, NF-kappaB expression, ameliorates BBB permeability and endothelial cell function, and protects rat brains against focal ischemia. Brain Res. 1321, 143–151.
Wu, B., Liu, M., Zhang, S., 2007. Dan Shen agents for acute ischaemic stroke. Cochrane Database Syst. Rev. 2. CD004295.
Yaghi, S., Furie, K.L., Viscoli, C.M., Kamel, H., Gorman, M., Dearborn, J., Young, L.H., Inzucchi, S.E., Lovejoy, A.M., Kasner, S.E., Conwit, R., Kernan, W.N., Investigators, I. T., 2018. Pioglitazone prevents stroke in patients with a recent transient ischemic attack or ischemic stroke: a planned secondary analysis of the IRIS trial (Insulin Resistance Intervention After Stroke). Circulation 137 (5), 455–463.
Zhang, B., Wang, B., Cao, S., Wang, Y., 2015. Epigallocatechin-3-Gallate (EGCG) attenuates traumatic brain injury by inhibition of Edema formation and oxidative stress. Korean J. Physiol. Pharmacol. 19 (6), 491–497.
Zheng, Q.H., Li, X.L., Mei, Z.G., Xiong, L., Mei, Q.X., Wang, J.F., Tan, L.J., Yang, S.B., Feng, Z.T., 2017. Efficacy and safety of puerarin injection in curing acute ischemic stroke: a meta-analysis of randomized controlled trials. Medicine ((Baltimore)) 96 (1), e5803.
Zhou, Z.Y., Huang, B., Li, S., Huang, X.H., Tang, J.Y., Kwan, Y.W., Hoi, P.M., Lee, S.M., 2018. Sodium tanshinone IIA sulfonate promotes endothelial integrity via regulating VE-cadherin dynamics and RhoA/ROCK-mediated cellular contractility and prevents atorvastatin-induced intracerebral hemorrhage in zebrafish. Toxicol. Appl. Pharmacol. 350, 32–42.
Zhou, L., Zuo, Z., Chow, M.S., 2005. Danshen: an overview of its chemistry, pharmacology, pharmacokinetics, and clinical use. J. Clin. Pharmacol. 45 (12), 1345–1359.